


# Aortic flow dynamics and stiffness in Loeys–Dietz syndrome patients: a comparison with healthy volunteers and Marfan syndrome patients

Aroa Ruiz-Muñoz <sup>1,2,3</sup>, Andrea Guala<sup>1,2,3\*</sup>, Jose Rodriguez-Palomares<sup>1,2,3</sup>, Lydia Dux-Santoy<sup>1</sup>, Luz Servato<sup>3</sup>, Angela Lopez-Sainz<sup>3</sup>, Lucia La Mura<sup>1,4</sup>, Chiara Granato<sup>3</sup>, Javier Limeres<sup>3</sup>, Teresa Gonzalez-Alujas<sup>3</sup>, Laura Galián-Gay<sup>3</sup>, Laura Gutiérrez<sup>3</sup>, Kevin Johnson<sup>5</sup>, Oliver Wieben<sup>5</sup>, Augusto Sao-Aviles<sup>1,3</sup>, Ignacio Ferreira-Gonzalez<sup>1,2,3,6,7</sup>, Arturo Evangelista<sup>1,2,3,7,8</sup>, and Gisela Teixido-Tura<sup>1,2,3</sup>

<sup>1</sup>Vall d'Hebron Institut de Recerca (VHIR), Barcelona, Spain; <sup>2</sup>CIBER-CV, Instituto de Salud Carlos III, Madrid, Spain; <sup>3</sup>Department of Cardiology, Hospital Universitari Vall d'Hebron, Paseo Vall d'Hebron 119-129, 08035 Barcelona, Spain; <sup>4</sup>Department of Advanced Biomedical Sciences, University Federico II, Naples, Naples, Italy; <sup>5</sup>Department of Medical Physics and Radiology, University of Wisconsin, Madison, WI, USA; <sup>6</sup>CIBER-ESP, Instituto de Salud Carlos III, Madrid, Spain; <sup>7</sup>Universitat Autònoma de Barcelona, Bellaterra, Spain; and <sup>8</sup>Instituto del Corazón. Quirónsalud-Teknon. Barcelona, Spain

Received 28 September 2020; editorial decision 23 March 2021

## Aims

To assess aortic flow and stiffness in patients with Loeys–Dietz syndrome (LDS) by 4D flow and cine cardiovascular magnetic resonance (CMR) and compare the results with those of healthy volunteers (HV) and Marfan syndrome (MFS) patients.

## Methods and results

Twenty-one LDS and 44 MFS patients with no previous aortic dissection or surgery and 35 HV underwent non-contrast-enhanced 4D flow CMR. In-plane rotational flow (IRF), systolic flow reversal ratio (SFRR), and aortic diameters were obtained at 20 planes from the ascending (AAo) to the proximal descending aorta (DAo). IRF and SFRR were also quantified for aortic regions (proximal and distal AAo, arch and proximal DAo). Peak-systolic wall shear stress (WSS) maps were also estimated. Aortic stiffness was quantified using pulse wave velocity (PWV) and proximal AAo longitudinal strain. Compared to HV, LDS patients had lower rotational flow at the distal AAo ( $P=0.002$ ), arch ( $P=0.002$ ), and proximal DAo ( $P<0.001$ ) even after adjustment for age, stroke volume, and local diameter. LDS patients had higher SFRR in the proximal DAo compared to both HV ( $P=0.024$ ) and MFS patients ( $P=0.015$ ), even after adjustment for age and local diameter. Axial and circumferential WSS in LDS patients were lower than in HV. AAo circumferential WSS was lower in LDS compared to MFS patients. AAo and DAo PWV and proximal AAo longitudinal strain revealed stiffer aortas in LDS patients compared to HV ( $P=0.007$ ,  $0.005$ , and  $0.029$ , respectively) but no differences vs. MFS patients.

## Conclusion

Greater aortic stiffness as well as impaired IRF and WSS were present in LDS patients compared to HV. Conversely, similar aortic stiffness and overlapping aortic flow features were found in Loeys–Dietz and Marfan patients.

## Keywords

Loeys–Dietz syndrome • Marfan syndrome • rotational flow • aortic stiffness • 4D flow CMR • pulse wave velocity

\* Corresponding author. Tel: +34 (9) 34 894 798; Fax: +34 (9) 32 746 063. E-mail: andrea.guala@yahoo.com

Published on behalf of the European Society of Cardiology. All rights reserved. © The Author(s) 2021. For permissions, please email: journals.permissions@oup.com.

## Introduction

Loeys–Dietz syndrome (LDS) is an autosomal-dominant hereditary connective tissue disorder (CTD) with widespread systemic involvement characterized by vascular alterations, skeletal manifestations, and craniofacial and cutaneous features.<sup>1</sup> This rare syndrome is caused by pathogenic variants in the genes related to the transforming growth factor- $\beta$  signalling pathway<sup>1,2</sup> and entails an increased risk of aneurysms and dissections.<sup>3</sup>

Marfan syndrome (MFS), a more common CTD caused by pathogenic variants in the *FBN1* gene, shares overlapping phenotypic features with LDS such as skeletal manifestations and aortic dilation.<sup>4,5</sup> Early studies reported shorter life expectancy for patients with LDS compared to patients with MFS,<sup>1</sup> with dissections occurring earlier and at smaller aortic diameters<sup>1,3</sup>; however, recent studies found similar prognoses in patients with LDS and MFS.<sup>6–8</sup> This discrepancy may be partially due to the relatively recent description of LDS and the wide variability and severity in patients with LDS, even among family members with the same pathogenic variant.<sup>6</sup>

In recent years, cardiovascular magnetic resonance (CMR) imaging has emerged as a potential tool to provide comprehensive information on aortic flow dynamics and stiffness. In particular, time-resolved three-dimensional phase-contrast CMR (4D flow CMR) permits both regional aortic biomechanics<sup>9</sup> and advanced haemodynamic characteristics<sup>10</sup> to be assessed with an unprecedented level of detail. Recent CMR studies in patients with MFS reported increased aortic stiffness<sup>9,11–14</sup> and altered rotational flow patterns and wall shear stress (WSS),<sup>15–19</sup> with all these abnormalities being present even in patients without aortic dilation.<sup>9,15</sup> Of note, increased aortic stiffness showed an independent value to stratify the risk of progressive aortic dilation, dissection, and need for aortic root replacement.<sup>20,21</sup> To the best of our knowledge, no previous studies had assessed aortic stiffness and haemodynamics in patients with LDS.

This study aims to assess aortic blood flow and aortic stiffness by 4D flow and cine CMR in patients with LDS and compare the results with those of healthy volunteers (HV) and patients with MFS.

## Methods

### Study population

Twenty-one genetically confirmed patients with LDS were prospectively and consecutively recruited from the Genetic Aortic Unit of the Vall d'Hebron Hospital. Exclusion criteria were age <18 years, previous aortic dissection or aortic surgery, significant aortic valve disease (>grade II aortic regurgitation or stenosis), and bicuspid aortic valve or contraindication for CMR. In order to compare the LDS and MFS populations, 44 patients with MFS were retrospectively identified from a cohort of 75 consecutive previously studied cases with MFS by excluding patients with aortic root diameter >46 mm and body surface area (BSA) >2.0 m<sup>2</sup> (i.e. the maximum values of these parameters in the LDS group). Thirty-five HV matched for age, sex, and BSA were also included for comparison. The study was approved by the institutional ethics committee and written informed consent was obtained from all participants.

### CMR protocol

CMR studies were performed on a 1.5-T Signa scanner (GE Healthcare, Waukesha, Wisconsin, USA). The protocol included double-oblique

balanced steady-state free-precession cine imaging to evaluate aortic diameter at the sinus of Valsalva (SoV), 2D phase-contrast images at the aortic valve to assess valve disease, and a 4D flow CMR study to analyse aortic flow dynamics, biomechanics, and regional diameter.

A radially-undersampled acquisition [PC-VIPR (phase-contrast vastly undersampled isotropic projection)] with five-point balanced velocity encoding<sup>22</sup> and retrospective ECG gating during free-breathing was used for 4D flow CMR imaging of the entire thoracic aorta. 4D flow CMR acquisitions were made using the following parameters: velocity encoding 200 cm/s, field of view 400 × 400 × 400 mm, acquisition matrix 160 × 160 × 160, voxel size 2.5 × 2.5 × 2.5 mm, and flip angle 8°. The dataset was reconstructed according to the nominal temporal resolution of each patient, ranging from 20 to 42 ms. Data were corrected for background phase from concomitant gradients, eddy currents, and trajectory errors of the 3D radial acquired k-space.<sup>22</sup> Brachial systolic (SBP) and diastolic (DBP) blood pressures were taken immediately after the CMR study.

### Aortic flow dynamics evaluation with 4D flow CMR

A 3D segmentation of the thoracic aorta was obtained from the angiogram derived from the 4D flow CMR using ITK-SNAP.<sup>23</sup> The aortic centreline was computed and several anatomical landmarks were defined (Figure 1B). Twenty equidistant planes of analysis were located between the sinotubular junction and the proximal descending aorta (DAo) at the level of the pulmonary artery bifurcation: 8 in the ascending aorta (AAo) (from the sinotubular junction to the first supra-aortic vessel), 4 in the arch (from the first to the third supra-aortic vessels), and 8 in the proximal DAo (Figure 1C).

Flow-dynamics characterization was obtained in each plane by means of custom-designed Matlab code (Mathworks, Natick, MA, USA). Systolic flow reversal ratio (SFRR) was calculated as the ratio of backward to forward volumes passing through the plane during systole. This parameter offers quantification of the magnitude of vortices rotating around an axis perpendicular to the centreline.<sup>24</sup> In-plane rotational flow (IRF) was quantified as the integral over the cross-section of the in-plane component of circulation, a parameter used in fluid dynamics to quantify flow rotation within a plane<sup>25</sup> at the systolic peak (Figure 1C). Both parameters were also quantified for aortic regions (proximal and distal AAo, arch and proximal DAo) by averaging them in all the planes pertaining to each region.

For each analysis plane, peak-systolic WSS vectors were calculated as previously described<sup>10,26</sup> and were decomposed into axial and circumferential components.<sup>27</sup> Lumen contours were aligned for all patients using the inner aortic curvature as a reference, and axial and circumferential WSS were averaged at eight regions around the contour at each analysis plane (left-outer, left, left-inner, inner, right-inner, right, right-outer, and outer) (Figure 1D). Population-averaged WSS maps were obtained for each of the three patient groups (i.e. LDS, MFS, and HV).

### Aortic mechanical properties

Mechanical properties of the aortic wall were characterized by an in-house Matlab code (MathWorks, Inc., Natick, MA, USA). Regional aortic pulse wave velocities (PWV) were computed separately from 4D flow CMR data in the AAo and DAo.<sup>9</sup> Velocity waveforms were extracted at 100 equally distributed analysis planes and transit time was calculated with the wavelet-based method, the most robust technique.<sup>28</sup> The AAo was here defined from the sinotubular junction to the third supra-aortic vessel and the DAo from the third supra-aortic vessel to the level of the diaphragm.

Proximal AAo longitudinal strain was computed by tracking the aortic valve throughout the cardiac cycle from a set of coronal and sagittal aortic valve cine images, as previously detailed.<sup>21</sup>

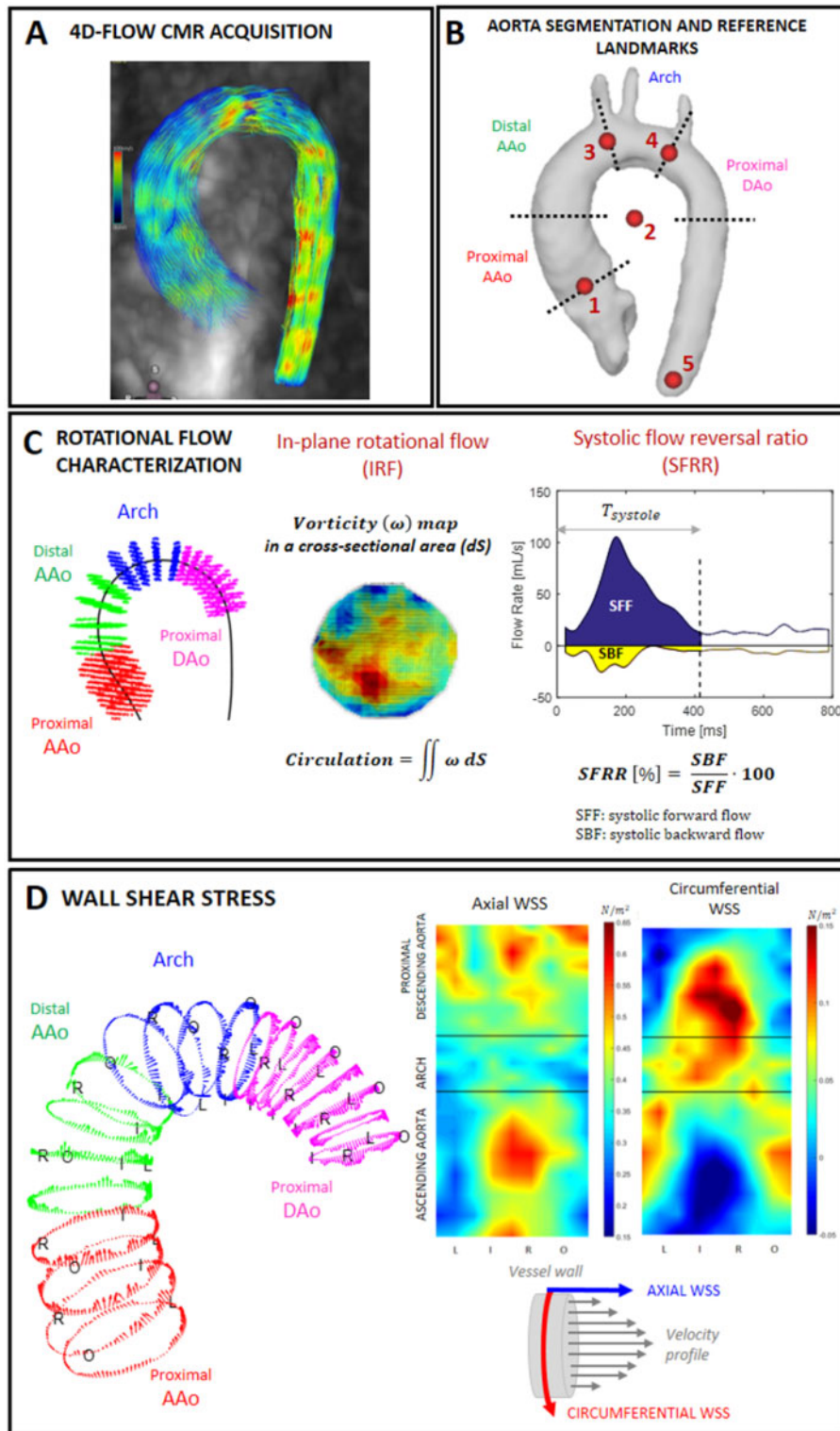


**Figure 1** Analysis planes and flow parameters calculated from 4D flow CMR (A). 3D aorta segmentation, aortic regions, centreline, and reference anatomical landmarks (B) at the sinotubular junction,<sup>1</sup> pulmonary artery bifurcation,<sup>2</sup> first<sup>3</sup> and third<sup>4</sup> supra-aortic trunks, and diaphragmatic level.<sup>5</sup> IRF and SFRR (C). WSS vectors (left panel) and, axial and circumferential WSS maps (right panel) (D).

## Aortic diameters

Three cusp-to-cusp aortic root diameters were quantified from double-oblique cine CMR acquisitions at end-diastole and the maximum was retained for analysis. Aortic root dilation was considered when z-score, based on age, BSA, and sex as reported by Devereux *et al.*,<sup>29</sup> was >2. Moreover, at each analysis plane, local aortic diameter was automatically extracted from the 4D flow CMR segmentation by computing the circle that best fit (least-squares method) the local segmentation of the aorta.

## Statistical analysis

Continuous variables are expressed as mean  $\pm$  standard deviation if they presented a normal distribution and as median [1st–3rd] quartiles otherwise. Categorical variables are presented as frequency (percentage). The Shapiro–Wilk test was used to assess distribution normality in LDS and Kolmogorov–Smirnov test in patients with MFS and HV. Differences between groups for continuous parameters were assessed by Student's *t*-test if normally distributed and Mann–Whitney *U* test otherwise. Chi-square test was used for categorical variables. Multivariate linear regression analyses with a backward selection procedure and multicollinearity test were used to identify statistically significant independent associations. Independent variables entered the model if  $P < 0.2$  on bivariate analysis and were progressively excluded if  $P > 0.1$ . A two-tailed *P*-value  $< 0.05$  was considered statistically significant. SPSS 21.0 (IBM SPSS Statistics, Chicago, IL, USA) was used for the analysis.

## Results

### Demographic and clinical characteristics

The demographic and clinical characteristics of the LDS, HV, and MFS groups are shown in Table 1, while regional aortic diameters are

shown in Figure 2. Patients with LDS presented pathogenic variants in the following genes: TGFBR1 in 13, TGFBR2 in 1, SMAD3 in 3, and TGFBR2 in 4. The cohort included 21 LDS patients from 12 familial cases. Eleven patients with LDS (55%) were not receiving medical treatment at the moment of the CMR study, 7 (35%) were treated with Losartan, and 2 (10%) received Atenolol. In the MFS group, 37% of patients were under no medical treatment, and 39% and 24% were treated with Losartan and Atenolol, respectively. None of the healthy subjects received any antihypertensive treatment. No differences in medical treatment were found between patients with LDS and MFS. No differences in age, sex, weight, BSA, blood pressure, heart rate, left-ventricular end-systolic, end-diastolic and stroke volumes, and ejection fraction were observed between patients with LDS and patients with MFS or HV. However, patients with MFS were taller than patients with LDS. Compared to HV, patients with LDS presented larger diameters at the SoV even after indexing for BSA or computing z-scores and at proximal AAO, even after indexing for BSA (Figure 2). Compared to patients with MFS, patients with LDS did not present differences in aortic root z-scores or in diameters at the SoV (Table 1) and other aortic levels, even after indexing for BSA (Figure 2).

## Aortic flow dynamics

### In-plane rotational flow

IRF (the in-plane projection of helical flow) at the 20 analysis planes in each group is shown in Figure 3A. IRF in the LDS and MFS groups showed similar behaviour, with values generally lower than HV, with the notable exception of the very proximal AAO. Interestingly, blood helical flow in patients with LDS and MFS transitioned from right-handed to left-handed rotation (i.e. positive to negative values) in the

**Table 1** Demographics in Loeys–Dietz (LDS) syndrome patients, Marfan (MFS) syndrome patients, and healthy volunteers (HV)

	LDS (N = 21)	HV (N = 35)	MFS (N = 44)	LDS vs. HV P-value	LDS vs. MFS P-value
Age [years]	34 [23; 48]	34 [30; 45]	37 [28; 45]	0.953	0.833
Men [N (%)]	6 (29%)	19 (54%)	6 (14%)	0.095	0.180
Weight [Kg]	65 [58; 75]	70 [61; 79]	63 [58; 70]	0.287	0.347
Height [cm]	168 [161; 180]	170 [163; 175]	173 [169; 181]	0.627	<b>0.022</b>
BSA [m <sup>2</sup> ]	1.80 [1.61; 1.89]	1.82 [1.67; 1.93]	1.75 [1.70; 1.84]	0.461	0.900
SBP [mmHg]	117 [107; 134]	122 [110; 135]	122 [110; 139]	0.210	0.290
DBP [mmHg]	76 [71; 79]	70 [60; 80]	71 [60; 82]	0.111	0.457
Stroke volume [mL]	87 [70; 96]	85 [67; 94]	85 [74; 97]	0.763	0.833
LV ejection fraction [%]	63 [60; 69]	64 [59; 68]	64 [56; 68]	0.814	0.769
HR [bpm]	61 [56; 73]	60 [56; 66]	61 [55; 72]	0.417	0.844
LVEDV [mL]	134 [110; 158]	134 [115; 149]	138 [125; 148]	0.858	0.243
LVESV [mL]	47 [34; 60]	51 [37; 59]	49 [43; 63]	0.756	0.268
SoV D [mm]	33 [31; 37]	29 [26; 32]	35 [32; 40]	<b>0.001</b>	0.332
SoV D/BSA [mm/m <sup>2</sup> ]	19 [17; 21]	16 [15; 18]	20 [18; 23]	<b>&lt;0.001</b>	0.351
SoV z-score	1.23 [0.78; 2.12]	−0.52 [−0.92; 0.38]	2.12 [0.95; 2.94]	<b>&lt;0.001</b>	0.157
<b>Antihypertensive treatment</b>				<b>0.000</b>	0.131
No treatment	11 (55%)	35 (100%)	14 (37%)		
Losartan	7 (35%)	0 (0%)	15 (39%)		
Atenolol	2 (10%)	0 (0%)	9 (24%)		

Values are median [first; third interquartile] or *n* (%). *P*-values refer to bivariate analyses.

Bold values highlight statistically-significant ( $P < 0.05$ ) associations.

BSA = body surface area, D = diameter, LVEDV and LVESV = end-diastolic and end-systolic left-ventricular volumes, respectively; HR = heart rate, SBP and DBP = systolic and diastolic blood pressure, respectively, SoV = sinus of Valsalva.



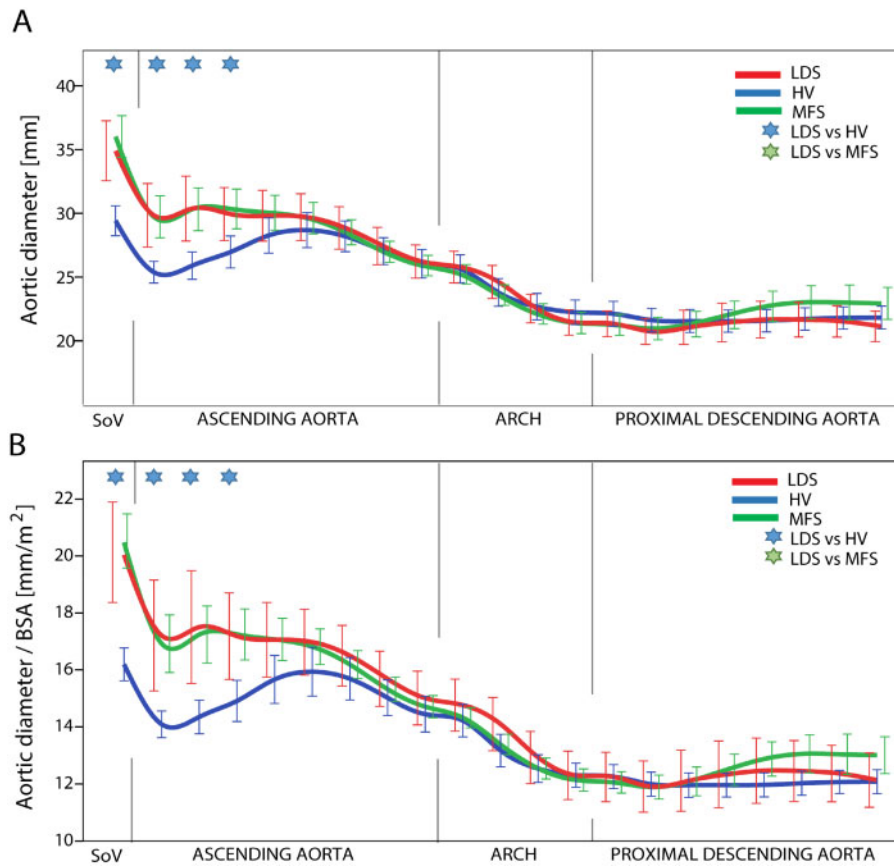


**Figure 2** Aortic diameters. Local diameters (top) and diameters indexed by BSA (bottom) at the SoV and 20 planes located between the sinotubular junction and proximal DAo. Red lines and boxplots present data for the LDS population, blue reports HV data, and green the MFS group. Blue and green markers represent statistically-significant differences ( $P < 0.05$ ) between LDS and HV and MFS populations, respectively, on bivariate analysis.

middle of the proximal DAo, in contrast to HV in whom there was not inversion of flow rotation direction (Figure 3A).

Median IRF values in each aortic region are shown in Table 2. Compared to HV, patients with LDS had lower rotational flow at the distal AAo, arch, and proximal DAo even on multivariate analysis corrected for age, stroke volume, and local diameter. On the other hand, no statistically-significant differences in IRF were found between patients with LDS and MFS on multivariate analysis corrected for age, stroke volume, and local diameter (Table 2).

### Systolic flow reversal ratio

SFRR at the 20 analysis planes and median values in each aortic region are presented in Figure 3B and Table 3, respectively. Patients with LDS had higher SFRR in the proximal DAo compared to both HV and patients with MFS, even after adjustment for age and local aortic diameter on multivariate linear regression analyses.

### WSS maps

Statistically-significant differences in axial WSS were found between patients with LDS and HV, with axial WSS being significantly lower in the outer region of the proximal AAo and in the inner region of the proximal DAo in patients with LDS syndrome (Figure 4A). On the

other hand, circumferential WSS was lower in LDS subjects compared with HV in the inner-right region of the distal AAo, and in a wide area in the arch and in mid-proximal DAo (Figure 4B).

Axial WSS was similar in the LDS and MFS groups (Figures 4A). In contrast, circumferential WSS was lower in LDS compared to MFS in the right-inner region of the AAo (Figure 4B).

## Aortic mechanical properties

Ascending and DAo PWV were higher in LDS compared to HV, even after adjustment for SoV diameter (Table 4). Conversely, no differences in AAo and DAo PWV were found between patients with LDS and MFS. Similarly, proximal aorta longitudinal strain was lower in LDS compared to HV but similar to that in MFS, even after adjustment for age. Of note, receiving antihypertensive treatment vs. receiving no antihypertensive treatment was not found to have an independent association with these biomechanical parameters in patients with LDS and MFS.

## Discussion

This study analysed blood flow characteristics and aortic stiffness by 4D flow and cine CMR in the thoracic aorta of adult patients

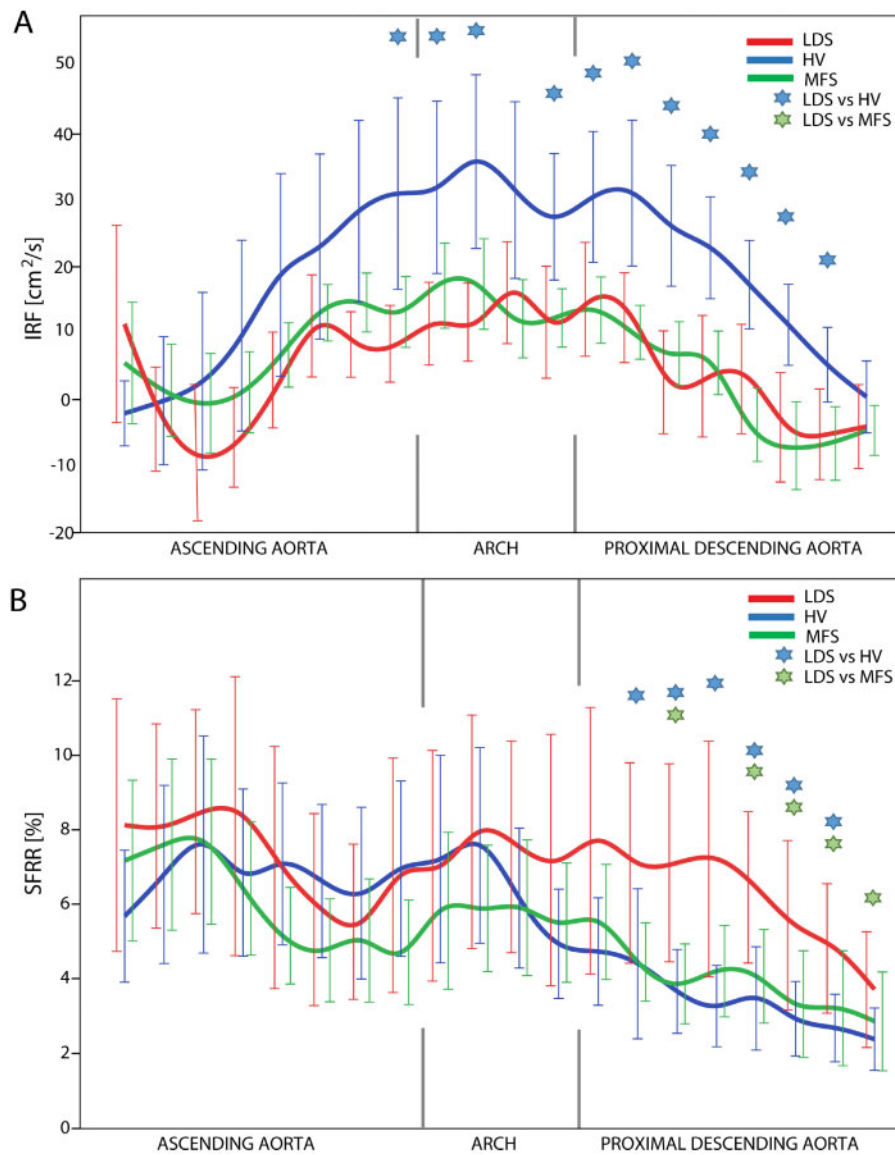


**Figure 3** Rotational flow patterns. IRF (A) and SFRR (B) at the 20 analysis planes. Red lines and boxplots present data for the LDS population, blue reports HV data, and green the MFS group. Blue and green markers represent statistically-significant differences ( $P < 0.05$ ) between LDS and HV and MFS groups, respectively, on bivariate analysis.

**Table 2** IRF in Loeyes–Dietz (LDS), MFS patients, and HVs

Aortic region	IRF LDS (N = 21)	IRF HV (N = 35)	IRF MFS (N = 44)	P-value LDS vs. HV	P-value LDS vs. MFS
Proximal AAo	−5.56 [−12.86; 5.45]	−2.73 [−8.92; 5.80]	−2.05 [−8.05; 10.69]	0.142	0.651
Distal AAo	6.41 [−1.09; 14.00]	14.82 [3.32; 44.80]	11.71 [3.75; 16.25]	<b>0.002</b>	0.152
Arch	10.96 [2.67; 19.42]	23.26 [13.52; 51.19]	13.79 [4.89; 25.05]	<b>0.002</b>	0.595
Proximal Dao	0.77 [−6.80; 14.55]	16.24 [6.10; 32.31]	3.56 [−3.47; 9.65]	<b>&lt;0.001</b>	0.507

Values are reported as median [first; third interquartile].

P-values are for multivariate linear regression analyses adjusted for age, stroke volume, and local aortic diameter. Bold values highlight statistically-significant ( $P < 0.05$ ) associations.

**Table 3** SFRR in Loey's–Dietz (LDS), MFS, and HVs

Aortic region	SFRR LDS (N = 21)	SFRR HV (N = 35)	SFRR MFS (N = 44)	LDS vs. HV P-value	LDS vs. MFS P-value
Proximal AAO	6.39 [4.25; 14.15]	5.32 [3.32; 9.09]	5.49 [3.14; 10.67]	0.708	0.387
Distal AAO	4.36 [2.03; 9.06]	4.71 [2.67; 10.35]	3.47 [2.23; 6.20]	0.650	0.261
Arch	5.58 [2.38; 13.31]	4.79 [2.57; 10.42]	4.99 [1.87; 6.87]	0.261	0.062
Proximal DAAo	5.64 [3.20; 9.63]	3.12 [1.26; 4.63]	3.15 [2.14; 4.59]	<b>0.024</b>	<b>0.015</b>

Values are reported as median [first; third interquartile].

P-values are for multivariate linear regression analyses adjusted for age and local aortic diameter. Bold values highlight statistically-significant ( $P < 0.05$ ) associations.

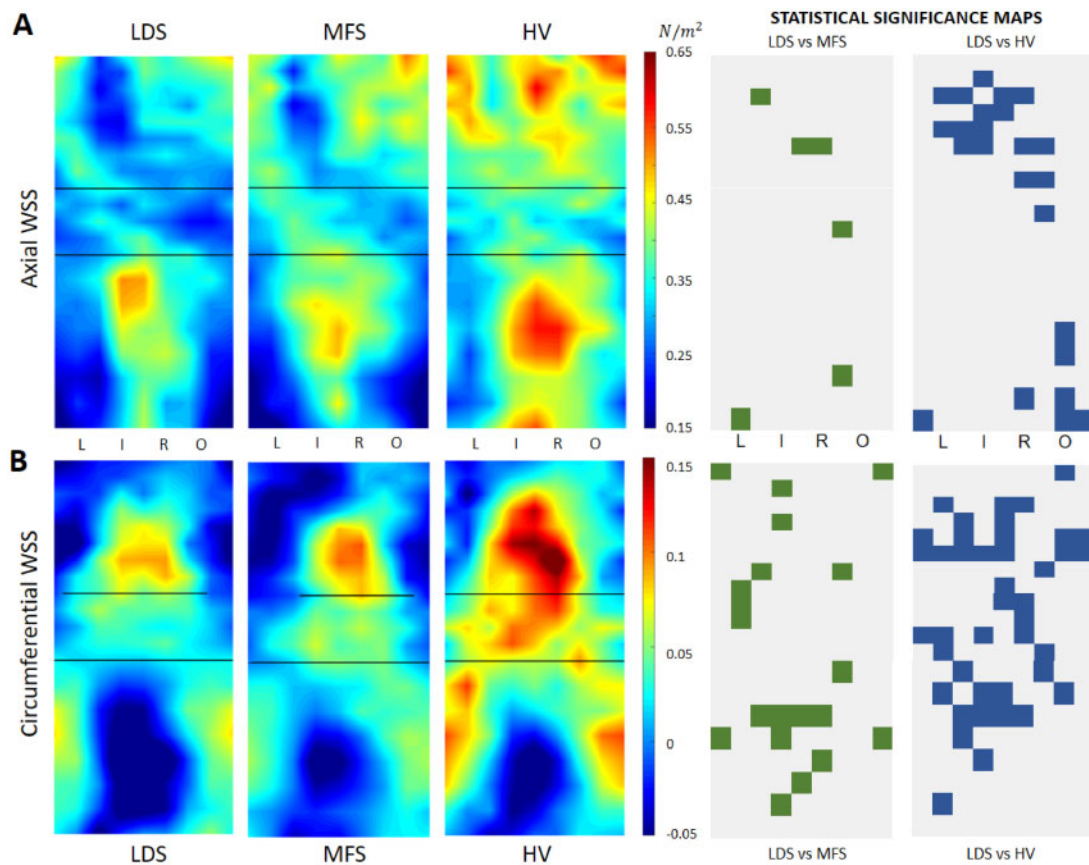


**Figure 4** Axial (A) and circumferential (B) WSS maps in patients with Loey's–Dietz (LDS) or MFS and HVs. Statistical significance ( $P < 0.05$ ) maps comparing patients with LDS vs. patients with MFS and patients with LDS vs. HV for axial (A) and circumferential (B) WSS. *I* = inner, *L* = left, *O* = outer, and *R* = right.

with LDS compared with patients with MFS and HV matched for age, sex, BSA, and blood pressure. The main findings of this work were that: ascending and descending aortic stiffness was greater in LDS than in HV but similar to patients with MFS; in-plane flow rotation and circumferential WSS in the distal AAO, arch and proximal DAAo of patients with LDS were lower than in HV; and vortices in the proximal DAAo of patients with LDS were characterized by higher SFRR compared to HV and patients with MFS.

To the best of our knowledge, this is the first study to analyse both flow dynamics and aortic biomechanics in a cohort of patients with LDS and compare them to patients with MFS and HV.<sup>20,30,31</sup>

### Aortic mechanical properties

Regional PWV in the ascending and DAAo were higher and AAO longitudinal strain was lower in patients with LDS compared to HV, thereby suggesting that patients with LDS had increased aortic stiffness. Of note, this increased aortic stiffness in LDS was found even in the

**Table 4** Ascending (AAo) and descending (DAo) aorta PWV and proximal AAo longitudinal strain in Loeys–Dietz (LDS), HVs, and Marfan (MFS) patients

Parameter	LDS (N = 21)	HV (N = 35)	MFS (N = 44)	LDS vs. HV P-value	LDS vs. MFS P-value
AAo PWV [m/s]	6.9 [5.8; 8.4]	4.9 [3.7; 6.2]	6.3 [5.3; 7.7]	<b>0.007<sup>a</sup></b>	0.370 <sup>a</sup>
DAo PWV [m/s]	9.0 [6.9; 11.1]	6.3 [5.0; 7.9]	8.8 [6.8; 12.6]	<b>0.005<sup>a</sup></b>	0.494 <sup>a</sup>
Proximal AAo longitudinal strain [%]	12.3 [7.7; 14.3]	15.4 [11.4; 16.9]	13.2 [9.4; 16.3]	<b>0.029<sup>b</sup></b>	0.182 <sup>b</sup>

Values are reported as median [interquartile range].

Bold values highlight statistically-significant ( $P < 0.05$ ) associations on multivariate analyses corrected for SoV diameter<sup>a</sup> or age<sup>b</sup>.

presence of relatively mild aortic root dilation [SoV z-score 1.23 (0.78; 2.12)], thus suggesting it may be an early characteristic of the disease. A similar result had been previously observed in patients with MFS,<sup>9,11,21</sup> where aortic stiffness predicted thoracic ascending and DAo dilation<sup>21,32</sup> and aortic events.<sup>21</sup> In our study, AAo and DAo PWV did not differ in patients with LDS and MFS. Very limited data are available on aortic stiffness in LDS. Indeed, in most studies, LDS was not analysed as an independent entity, but included together with MFS and Ehlers–Danlos syndrome patients in cohorts of individuals with CTDs.<sup>20,30,31</sup> Merlocco *et al.*<sup>31</sup> found that in children and young adults with CTD, aortic stiffness measured by CMR progressively increased with age and with rates of change only slightly higher than the normal population. Prakash *et al.*<sup>20</sup> related greater aortic stiffness with higher rates of surgical aortic replacement and aortic root dilation in children and young adults with CTD.

## Aortic flow dynamics

In this study, patients with LDS were observed to have less right-handed rotational flow at the distal AAo, arch and proximal DAo compared to healthy controls. This suggests that these patients are deficient in physiological helical flow, which is a flow organization particularly efficient in limiting energy dissipation and possibly protecting arteries from atherosclerosis, thrombosis, and intimal hyperplasia.<sup>33</sup> It is worth noting that such an abnormality was also present in patients with MFS, as previously reported.<sup>15</sup>

In contrast to MFS and HV, patients with LDS presented higher SFRR (systolic backward flow) in the proximal DAo. However, this increase in SFRR was small compared to that reported in other conditions such as bicuspid aortic valve disease.<sup>10,34–37</sup> For example, Rodriguez-Palomares *et al.*<sup>10</sup> found the SFRR at mid-AAo of patients with bicuspid aortic valve to be around 20%. Conversely, SFRR at the proximal DAo was 5.64% [3.20; 9.63] in LDS and 3.15 [2.14; 4.59] in patients with MFS. Only prospective longitudinal studies may establish whether this increase in SFRR observed in the proximal DAo of patients with LDS is clinically significant.

Regarding the interaction between flow abnormalities and stress at the aortic wall, substantial differences in WSS were found on comparing LDS with HV, while discrepancies with MFS were minor. Of note, altered WSS has been related to aortic wall disorganization and disruption,<sup>38</sup> and prospective studies in MFS showed that the alteration in WSS in the proximal DAo tended to worsen with disease progression.<sup>18</sup>

## Comparison of LDS and MFS

No significant differences were found between LDS and MFS in terms of AAo and DAo PWV and proximal AAo longitudinal strain, and only limited differences were unveiled regarding aortic flow abnormalities, despite both groups of patients with LDS and MFS presenting substantial differences in aortic biomechanics and flow dynamics compared with HV. These abnormalities—altered aortic rotational flow and WSS and increased aortic stiffness—may represent a common expression of CTD, and may concur with studies reporting similar prognoses in patients with LDS and MFS.<sup>6–8</sup> However, these findings may be valid only for adult patients with LDS similar to those included in the present study, with no previous aortic dissection or aortic surgery and non-severe aortic root dilation, which might represent a subgroup of LDS with relatively mild disease severity.<sup>1,2</sup>

## Limitations

The inclusion of adults with no previous aortic surgery or dissection resulted in a cohort of relatively mildly-affected individuals in terms of aortic diameter and in a greater percentage of women. These characteristics of the present cohort may limit the extrapolation of the results to LDS presenting more severe affectations and may be less robust in men than in women. However, the identification of additional markers of aortic risk beyond aortic diameters might be especially useful in non-advanced stages of the disease, as it is the cohort included in the present study. The cross-sectional nature of the study implies the impossibility of supporting causal relationships among variables, which should be addressed in future longitudinal studies.

Considering the heterogeneous genetic background of the LDS population and the relatively low number of subjects included, it was not possible to analyse flow dynamics and aortic biomechanics in patients with LDS separately for each pathogenic variant or type of medical treatment. Furthermore, although our centre is a reference hospital for heritable thoracic aortic diseases in Spain, it was not possible to include only index cases of LDS due to the limited incidence of the disease.

## Conclusions

Greater aortic stiffness as well as impaired IRF and circumferential WSS were present in patients with LDS compared to HVs. In contrast, similar aortic stiffness and overlapping aortic flow features were found in patients with Loeys–Dietz and MFSs.



## Acknowledgement

The authors are grateful to Christine O'Hara and Hannah Cowdrey for English revision.

## Data availability

The data that support the findings of this study are available from the corresponding authors upon reasonable request.

## Funding

This study was funded by La Marató de TV3 (project number 20151330) and Instituto de Salud Carlos III through the project PI17/00381. Guala A. received funding from the Spanish Ministry of Science, Innovation and Universities (IJC2018-037349-I). Dr. La Mura L. was supported by a research grant provided by the Cardiopath PhD programme.

**Conflict of interest:** K.M. Johnson received a research grant from GE Healthcare and from Myocardial Solutions through The University of Wisconsin-Madison (no personal compensation) and holds a consulting agreement with Vertex Pharmaceuticals. O.W. received a research grant from GE Healthcare through The University of Wisconsin-Madison (no personal compensation). The other authors report no conflicts.

## References

- Loeys BL, Schwarze U, Holm T, Callewaert BL, Thomas GH, Pannu H *et al.* Aneurysm syndromes caused by mutations in the TGF- $\beta$  receptor. *N Engl J Med* 2006;**355**:788–98.
- Loeys BL, Chen J, Neptune ER, Judge DP, Podowski M, Holm T *et al.* A syndrome of altered cardiovascular, craniofacial, neurocognitive and skeletal development caused by mutations in TGFBR1 or TGFBR2. *Nat Genet* 2005;**37**:275–81.
- Maccarrick G, Black IJ, Bowdin S, El-Hamamsy I, Frischmeyer-Guerrero PA, Guerrero AL *et al.* Loays–Dietz syndrome: a primer for diagnosis and management. *Genet Med* 2014;**16**:576–87.
- Brown OR, DeMots H, Kloster FE, Roberts A, Menashe VD, Beals RK. Aortic root dilatation and mitral valve prolapse in Marfan's syndrome: an echocardiographic study. *Circulation* 1975;**52**:651–7.
- Lindsay ME, Dietz HC. Lessons on the pathogenesis of aneurysm from heritable conditions. *Nature* 2011;**473**:308–16.
- Jondeau G, Ropers J, Regalado E, Braverman A, Evangelista A, Teixido G *et al.* Montalcino Aortic Consortium. International registry of patients carrying TGFBR1 or TGFBR2 mutations: results of the MAC (Montalcino Aortic Consortium). *Circ Cardiovasc Genet* 2016;**9**:548–58.
- Mühlstädt K, De Backer J, von Kodolitsch Y, Kutsche K, Muiño Mosquera L, Brickwedel J *et al.* Case-matched comparison of cardiovascular outcome in Loays–Dietz syndrome versus Marfan syndrome. *JCM* 2019;**8**:2079.
- Teixido-Tura G, Franken R, Galuppo V, García-Moreno LG, Borregan M, Mulder BJM *et al.* Heterogeneity of aortic disease severity in patients with Loays–Dietz syndrome. *Heart* 2016;**102**:626–32.
- Guala A, Rodriguez-Palmares J, Dux-Santoy L, Teixido-Turà G, Maldonado G, Galian L *et al.* Influence of aortic dilation on the regional aortic stiffness of bicuspid aortic valve assessed by 4-dimensional flow cardiac magnetic resonance: comparison with Marfan syndrome and degenerative aortic aneurysm. *JACC Cardiovasc Imaging* 2019;**12**:1020–9.
- Rodriguez-Palmares J, Dux-Santoy L, Guala A, Kale R, Maldonado G, Teixido-Turà G *et al.* Aortic flow patterns and wall shear stress maps by 4D-flow cardiovascular magnetic resonance in the assessment of aortic dilatation in bicuspid aortic valve disease. *J Cardiovasc Magn Reson* 2018;**20**:28. doi: 10.1186/s12968-018-0451-1
- Teixido-Turà G, Redheuil A, Rodriguez-Palmares J, Gutiérrez L, Sánchez V, Forteza A *et al.* Aortic biomechanics by magnetic resonance: early markers of aortic disease in Marfan syndrome regardless of aortic dilatation? *Int J Cardiol* 2014;**171**:56–61.
- Westenberg JJM, Scholte AJHA, Vaskova Z, Geest RVD, Groenink M, Labadie G *et al.* Age-related and regional changes of aortic stiffness in the Marfan syndrome: assessment with velocity-encoded MRI. *J Magn Reson Imaging* 2011;**34**:526–31.
- Hirata K, Triposkiadis F, Sparks E, Bowen J, Wooley CF, Boudoulas H. The Marfan syndrome: abnormal aortic elastic properties. *J Am Coll Cardiol* 1991;**18**:57–63.
- Salvi P, Grillo A, Marelli S, Gao L, Salvi L, Viecra M *et al.* Aortic dilatation in Marfan syndrome: role of arterial stiffness and fibrillin-1 variants. *J Hypertens* 2018;**36**:77–84.
- Guala A, Teixido-Tura G, Dux-Santoy L, Granato C, Ruiz-Muñoz A, Valente F *et al.* Decreased rotational flow and circumferential wall shear stress as early markers of descending aorta dilation in Marfan syndrome: a 4D flow CMR study. *J Cardiovasc Magn Reson* 2019;**21**:1–11. doi: 10.1186/s12968-019-0572-1
- Wang HH, Chiu HH, Tseng WYI, Peng HH. Does altered aortic flow in Marfan syndrome relate to aortic root dilatation? *J Magn Reson Imaging* 2016;**44**:500–8.
- Geiger J, Markl M, Herzer L, Hirtler D, Loeffelbein F, Stiller B *et al.* Aortic flow patterns in patients with Marfan syndrome assessed by flow-sensitive four-dimensional MRI. *J Magn Reson Imaging* 2012;**35**:594–600.
- Geiger J, Hirtler D, Gottfried K, Rahman O, Bollache E, Barker AJ *et al.* Longitudinal evaluation of aortic hemodynamics in Marfan syndrome: new insights from a 4D flow cardiovascular magnetic resonance multi-year follow-up study. *J Cardiovasc Magn Reson* 2017;**19**:11. doi: 10.1186/s12968-017-0347-5
- Van der Palen RLF, Barker AJ, Bollache E, Garcia J, Rose MJ, Van Ooij P *et al.* Altered aortic 3D hemodynamics and geometry in pediatric Marfan syndrome patients. *J Cardiovasc Magn Reson* 2017;**19**:30.
- Prakash A, Adlakha H, Rabideau N, Hass CJ, Morris SA, Geva T *et al.* Segmental aortic stiffness in children and young adults with connective tissue disorders. *Circulation* 2015;**132**:595–602.
- Guala A, Teixido-Turà G, Rodriguez-Palmares J, Ruiz-Muñoz A, Dux-Santoy L, Villalva N *et al.* Proximal aorta longitudinal strain predicts aortic root dilation rate and aortic events in Marfan syndrome. *Eur Heart J* 2019;**40**:2047–55.
- Johnson KM, Lum DP, Turski PA, Block WF, Mistretta CA, Wieben O. Improved 3D phase contrast MRI with off-resonance corrected dual echo VIPR. *Magn Reson Med* 2008;**60**:1329–36.
- Yushkevich PA, Piven J, Hazlett HC, Smith RG, Ho S, Gee JC *et al.* User-guided 3D active contour segmentation of anatomical structures: significantly improved efficiency and reliability. *Neuroimage* 2006;**31**:1116–28.
- Bensalah MZ, Bollache E, Kachenoura N, Giron A, De Cesare A, Macron L *et al.* Geometry is a major determinant of flow reversal in proximal aorta. *Am J Physiol–Heart Circ Physiol* 2014;**306**:1408–16.
- Hess AT, Bissell MM, Glaze SJ, Pitcher A, Myerson S, Neubauer S *et al.* Evaluation of circulation,  $\Gamma$ , as a quantifying metric in 4D flow MRI. *J Cardiovasc Magn Reson* 2013;**15**:E36.
- Stalder AF, Russe MF, Frydrychowicz A, Bock J, Hennig J, Markl M. Quantitative 2D and 3D phase contrast MRI: optimized analysis of blood flow and vessel wall parameters. *Magn Reson Med* 2008;**60**:1218–31.
- Dux-Santoy L, Guala A, Teixido-Turà G, Ruiz-Muñoz A, Maldonado G, Villalva N *et al.* Increased rotational flow in the proximal aortic arch is associated with its dilation in bicuspid aortic valve disease. *Eur Heart J Cardiovasc Imaging* 2019;**20**:1407–17.
- Bargiotas I, Mousseaux E, Yu WC, Venkatesh BA, Bollache E, De Cesare A *et al.* Estimation of aortic pulse wave transit time in cardiovascular magnetic resonance using complex wavelet cross-spectrum analysis. *J Cardiovasc Magn Reson* 2015;**17**:65. doi: 10.1186/s12968-015-0164-7
- Devereux RB, De Simone G, Arnett DK, Best LG, Boerwinkle E, Howard BV *et al.* Normal limits in relation to age, body size and gender of two-dimensional echocardiographic aortic root dimensions in persons >15 years of age. *Am J Cardiol* 2012;**110**:1189–94.
- Akazawa Y, Motoki N, Tada A, Yamazaki S, Hachiya A, Matsuzaki S *et al.* Decreased aortic elasticity in children with Marfan syndrome or Loays–Dietz syndrome. *Circ J* 2016;**80**:2369–75.
- Merlocco A, Lacro RV, Gauvreau K, Rabideau N, Singh MN, Prakash A. Longitudinal changes in segmental aortic stiffness determined by cardiac magnetic resonance in children and young adults with connective tissue disorders (the Marfan, Loays–Dietz, and Ehlers-Danlos Syndromes, and Nonspecific Connective Tissue Disorder). *Am J Cardiol* 2017;**120**:1214–9.
- Nollen GJ, Groenink M, Tijssen JGP, Van Der Wall EE, Mulder BJM. Aortic stiffness and diameter predict progressive aortic dilatation in patients with Marfan syndrome. *Eur Heart J* 2004;**25**:1146–52.
- Liu X, Sun A, Fan Y, Deng X. Physiological significance of helical flow in the arterial system and its potential clinical applications. *Ann Biomed Eng* 2015;**43**:3–15.
- Lorenz R, Bock J, Barker AJ, Von Knobelsdorff-Brenkenhoff F, Wallis W, Korvink JG *et al.* 4D flow magnetic resonance imaging in bicuspid aortic valve disease demonstrates altered distribution of aortic blood flow helicity. *Magn Reson Med* 2014;**71**:1542–53.
- Bissell MM, Loudon M, Hess AT, Stoll V, Orchard E, Neubauer S *et al.* Differential flow improvements after valve replacements in bicuspid aortic valve disease: a cardiovascular magnetic resonance assessment. *J Cardiovasc Magn Reson* 2018;**20**:1–10. doi: 10.1186/s12968-018-0431-5
- Hope MD, Hope TA, Crook SES, Ordovas KG, Urbani TH, Alley MT *et al.* 4D flow CMR in assessment of valve-related ascending aortic disease. *JACC Cardiovasc Imaging* 2011;**4**:781–7.
- Meierhofer C, Schneider EP, Lyko C, Hutter A, Martinoff S, Markl M *et al.* Wall shear stress and flow patterns in the ascending aorta in patients with bicuspid aortic valves differ significantly from tricuspid aortic valves: a prospective study. *Eur Heart J Cardiovasc Imaging* 2013;**14**:797–804.
- Guzzardi DG, Barker AJ, Van Ooij P, Malaisrie SC, Puthumana JJ, Belke DD *et al.* Valve-related hemodynamics mediate human bicuspid aortopathy: insights from wall shear stress mapping. *J Am Coll Cardiol* 2015;**66**:892–900.